

Abstract

In the 21st century the main cause of death is heart disease and cancer; accounting for almost 70% of total deaths. Every year almost 14 millions new cancer cases are registered, with over 8 million deaths annually. There are over 100 different types of cancer with the most common adult tumours affecting the lungs, liver, stomach, large intestine and breast. Five year survival rates can be as low as 10% for cancers of the lungs, liver and pancreas.

Surgery is the primary method of treatment for isolated, solid tumors, but is usually followed by chemo- or radio-therapy. However, the side effects of such adjuvant therapies can be severe, and new non – invasive methods of treatment are desperately sought. One such option is photodynamic therapy (PDT) in which a light source is combined with a photosensitizer to destroy abnormal cells. The interaction of light with the organic molecule leads to excitation and the transference of energy into an oxygen molecule in the ground state which results in the formation of an excited singlet oxygen molecule. Those organic photosensitizers currently in use have a number of disadvantages: (i) They do not have optimal optical properties for excitation, (ii) they exhibit absorption bands in the visible region where penetration of human tissue is highly limited, (iii) they exhibit low absorption coefficients which results in high doses of visible radiation. To counteract these deficiencies research is underway to try to replace organic photosensitizers with noble metal nanoparticles which exhibit more desirable optical properties. In this review article we present the roles that noble metal nanoparticles could play in PDT, and various methods of detection of the resulting singlet oxygen.

1. The discovery of photodynamic therapy

Porphyrins were first tested on humans as early as 1913 when Friedrich Meyer – Betz found that application of haematoporphyrin to his own skin resulted in pain in the light exposed areas [Meyer–Betz, 1913]. In the 1950s a haematoporphyrin derivative (HPD; Figure 1) was obtained by treating haematoporphyrins with acetic and sulphuric acids [Schwartz *et al.*, 1955] which was found to localize to tumours and emit fluorescence [Lipson *et al.*, 1961; Lipson & Baldes, 1960]. Whilst initially HPD showed promise as a diagnostic tool, it was later postulated that such porphyrins could exhibit phototoxic properties and might be able to kill cancer cells [Diamond *et al.*, 1972]. *In vivo* tests subsequently showed that porphyrins could delay the growth of gliomas implanted in rats; tumour growth could be stopped for 10 – 20 days, however the deeper regions of the tumour began to grow again after that time. Later work reported the possibility of applying HPD in conjunction with red light to eradicate mammary tumor growth in mice [Dougherty *et al.*, 1975]. In same year it was also shown that light activated HPD could eliminate bladder carcinoma in mouse [Kelly *et al.*, 1975]. The same group showed the first tests of light activated HPD in a human patient with bladder cancer [Kelly & Snell, 1976]. These tests indicated that there was slower tumor growth and tumor necrosis in the areas which received PDT. Following this seminal experiment, other teams applied PDT to lung tumours [Hayata *et al.*, 1982; Balchum *et al.*, 1984], gastric carcinomas [Hayata *et al.*, 1985], brain tumors [Sandeman, 1986; Hillet *et al.*, 1990; Popovic *et al.*, 1996; Rosenthal *et al.*, 2001], head and neck tumours [Schweitzer, 1990; Biel, 1998] and colorectal cancers [Mikvy *et al.*, 1998].

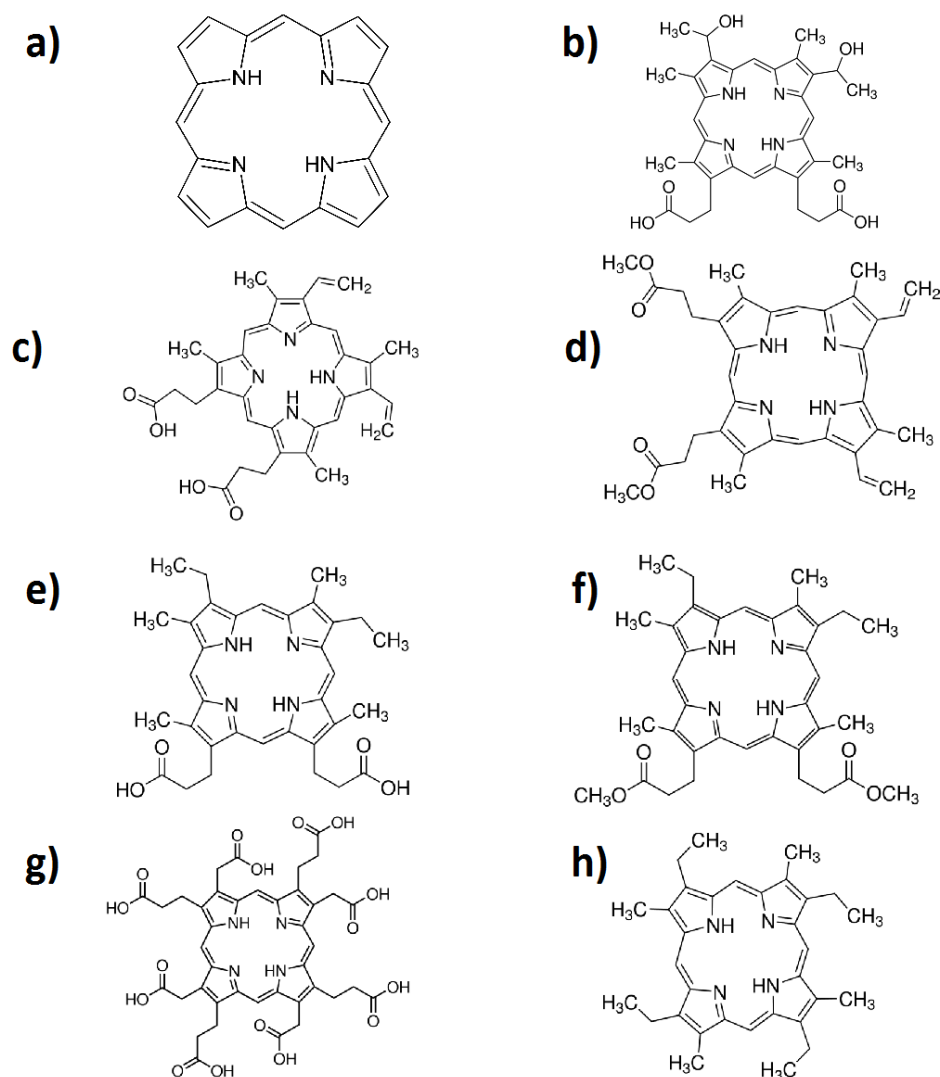


Fig. 1. Structural formulas of porphyrin, hematoporphyrin and hematoporphyrins derivative (HPD): a) porphyrin, b) hematoporphyrin, c) protoporphyrin IX, d) protoporphyrin IX diethyl ester, e) mesoporphyrin, f) mesoporphyrin diethyl ester, g) Uroporphyrin and h) Etioporphyrin.

2. Photodynamic processes and detection of singlet oxygen

PDT leads to tumour destruction by the generation of singlet oxygen. This singlet oxygen can either kill the tumor cell directly, or damage tumor associated vasculature. Furthermore, PDT can activate an immune response against the tumour, and most likely a combination of all three factors is required for effective tumor treatment.

After light absorption by a photosensitizer oxygen is transformed from ground singlet state to a short – lived excited singlet state. Due to non – radiative transition it is possible to then change multiplicities from singlet to long – lived triplet state. The excited photosensitizer in the triplet state can then decay via two types of process (see Fig. 2). It could produce radicals and radical ions in its surroundings (type I), or all of the energy could be transferred to an oxygen molecule in the ground state which leads to a form of singlet excited oxygen molecule (type II). Both processes occur simultaneously and the ratio between the type I and type II processes depends on the specific photosensitizer. It is estimated that

the average life time of an excited oxygen molecule is shorter than 0.04 μ s. Therefore it can act in a radius of 0.02 μ m.

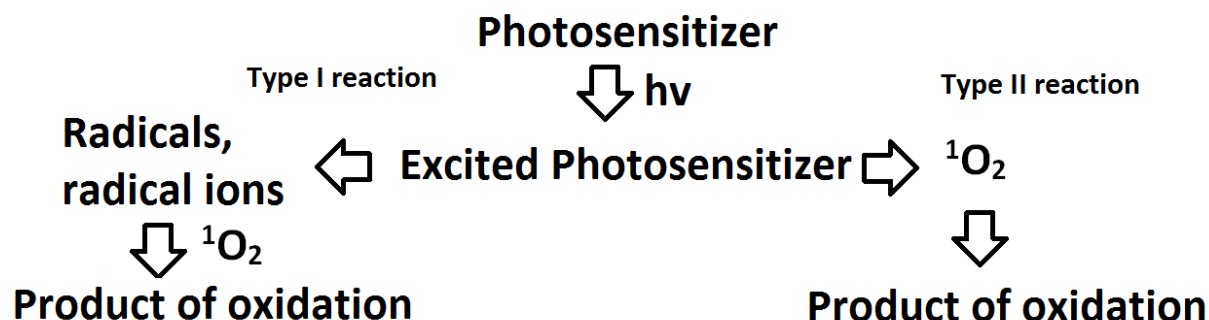
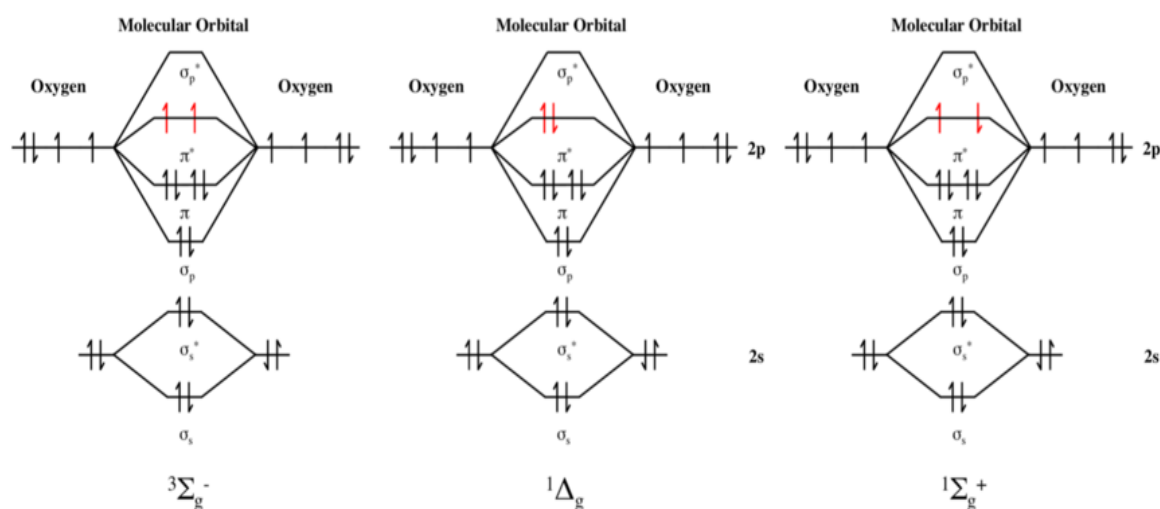


Fig. 2. Scheme presenting two type of mechanism in photodynamic process.

Singlet oxygen $^1\text{O}_2$ is a high energy form of oxygen, and far more reactive than oxygen in the ground triplet state. The excited singlet state has an energy level 94.29kJ/mol above the triplet ground state. This amount of energy corresponds to a transition in the near-infrared at ~ 1270 nm. Therefore one the method of detection of singlet oxygen involves a direct phosphorescence measurement at 1270nm.



Other methods are based on the interaction between singlet oxygen molecules and a substance sensitive to oxygen. Depending upon the exact nature of the effect on the sensor molecule, the change in structure could be monitored by different spectroscopic techniques such as NMR, EPR, UV-Vis absorption, or fluorescence. An example of this type of sensor compound is 9,10-Diphenylanthracene (DPA). In the presence of singlet oxygen could be observed decrease peak at 355nm which is proportional to singlet oxygen generation in system [J. Biol. Chem. 1992, 267, 13425-13433]. However, the main disadvantages of DPA as a singlet oxygen sensor is its poor solubility in water, although it is soluble in organic solvents such as benzene, toluene, or DMSO. A number of DPA derivatives have been

synthesized mainly aiming at improving the poor solubility. One of the most commonly used is 9,10-Anthracenediyl-bis(methylene)dimalonic acid (ABDA) which reacts irreversibly with singlet oxygen, inducing a reduction in the ABDA absorption band around 382 nm (see Figure 4). Another derivative, 9, 10-anthracenedipropionic acid (ADPA) shows a decrease in the absorption peak ADPA at 400nm upon reaction with singlet oxygen. Other DPA derivatives include Anthracene-9,10-diyl diethyl disulfate (EAS), anthracene-9,10-bisethanesulfonic acid (AES), anthracene-9,10-divinylsulfonate (AVS), bis-9,10-anthracene-(4-trimethyl-phenylammonium)dichloride (BPAA), N,N0-di-(2,3-dihydroxypropyl)-9,10-anthracene- dipropanamide (DHPA), and sodium 1,3-cyclohexadiene- 1,4-diethanoate (CHDDE) [Martines et al., 2000; Martinez et al., 2004; Botsivall et al., 1979; Nardello et al., 2005; Nardello et al., 1997; Martinez et al., 2006; Nardello et al., 1996].

Another widely used compound for spectrophotometrically detection of singlet oxygen is 1,3-diphenylisobenzofuran – DPBF. In the presence of singlet oxygen, DPBF immediately forms an unstable endoperoxide which decomposes to 1,2-dibenzoylbenzene. DPBF exhibits a strong absorption band at 415nm, and the decreasing signal is proportional to the amount of formed singlet oxygen.

Selected methods of singlet oxygen detection

Type of method	Sensor molecule		Changes caused by singlet oxygen
Absorption	9,10-Diphenylanthracene	DPA	Decrease peak at 355nm
Absorption	9,10-Anthracenediyl-bis(methylene)dimalonic acid	ABDA	Decrease peak at 382nm
Absorption	9, 10-anthracenedipropionic acid	ADPA	Decrease peak at 400nm
Absorption	anthracene-9,10-bisethanesulfonic acid	AES	Decrease peak at 360, 378 and 400nm
Absorption	1,3-diphenylisobenzofuran	DPBF	Decrease peak at 415nm
Phosphorescence	Singlet oxygen		Phosphorescence at 1067nm
Fluorescence	9-[2-(3-carboxy-9,10-diphenyl)anthryl]-6-hydroxy-	DPAX	Fluorescent endoperoxide formation
Fluorescence	3H-xanthen-3-one		
Fluorescence	9-[2-(3-carboxy-9,10-dimethyl) anthryl]-6-	DMAX	Fluorescent endoperoxide formation
Fluorescence	hydroxy-3H-xanthen-3-one		
Fluorescence	1,3-diphenylisobenzofuran	DPBF	Decrease fluorescence intensity
Fluorescence	Singlet Oxygen Sensor Green	SOSG	Strong green fluorescence
Chemiluminescence	2-methyl-6-phenyl- 3,7-dihydroimidazo	CLA	Strong chemiluminescence
	[1,2-a] pyrazin-3-one		
NMR	Cyclohexene		Change in NMR spectrum
EPR	2,2,6,6-tetramethylpiperidine	TEMP	Change in EPR spectrum

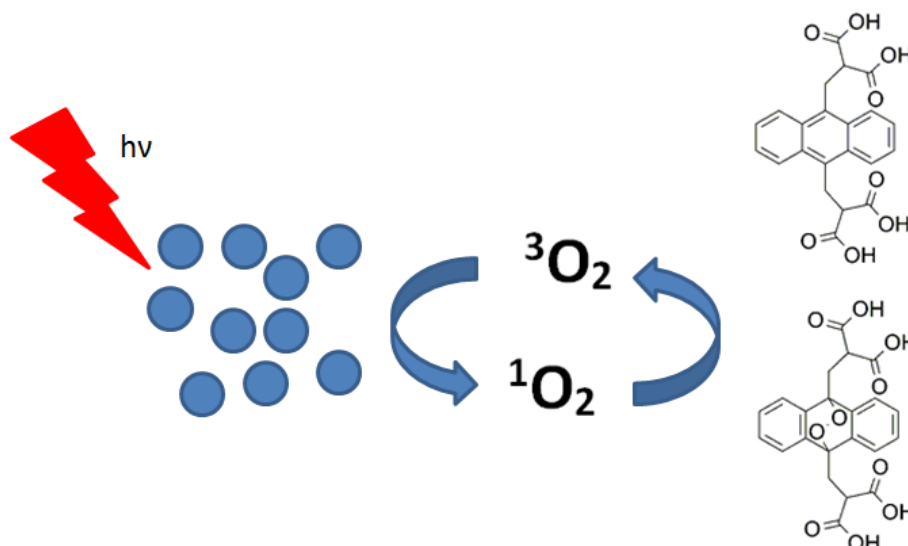


Fig. 4. Scheme showing the method of singlet oxygen detection with ABDA molecule as sensor.

Fluorescence measurements may also be used in the case when singlet oxygen interacts with a fluorescence probe leading to changes in fluorescence intensity, wavelength, quantum yield, or fluorescence lifetime. Historically, the first fluorescence probe used for singlet oxygen detection was 9-[2-(3-carboxy-9,10-diphenyl)anthryl]-6-hydroxy-3H-xanthen-3-one (DPAX). DPAX is not fluorescent until it interacts with singlet oxygen and forms the endoperoxide (DPAX-EPs) which is strongly fluorescent and has a high quantum yield [Umezawa et al., 1999]. However, DPAX can not be used in acidic environments. A similar molecule, 9-[2-(3-carboxy-9,10-dimethyl)anthryl]-6-hydroxy-3H-xanthen-3-one (DMAX), is also only fluorescent in its endoperoxide does form, but is much more sensitive and less hydrophobic, and can therefore be applied in biological samples [Tanaka et al., 2001].

In recent years, the most commonly used fluorescence probe is the Singlet Oxygen Sensor Green (SOSG) commercialized by Invitrogen/Molecular Probes. The indicator initially exhibits weak blue fluorescence, but in the presence of singlet oxygen emits a green fluorescence when excited at 504nm [Flors et al., 2006].

In comparison with organic compounds rare earth chelate complexes exhibit larger Stokes shifts and sharper emission curves when used for singlet oxygen detection. The most commonly used rare Earths chelates use terbium and europium (Eu^{3+} , Tb^{3+}). One example of a rare earth complex used to detect singlet oxygen is [40-(10-methyl-9-anthryl)-2,20:60,200-terpyridine-6,600-diyl] bis(methylenetrinitrilo) tetrakis(acetate)- Eu^{3+} (MTTA- Eu^{3+}) with the limit of detection reported to be 3.8nmol/dm^3 [Song et al., 2006]. However, a second probe, N,N,N',N'-[2,6-bis-(30-aminomethyl-10-pyrazolyl)-4-(900-anthryl)pyridine]tetrakis(acetate)- Tb^{3+} (PATA- Tb^{3+}) exhibits improved physicochemical properties such as high water solubility, wide pH applicable range and long lifetime of fluorescence, although the limit of detection for this system was estimated to be on 10.8nmol/dm^3 [Tan et al., 2006].

Despite such promising properties, the main disadvantage with rare earth probes is that they need UV light excitation, which could damage delicate biological systems. It is possible to shift excitation light to a longer wavelength using Rhenium in complexes such as: $\text{Re}(\text{CO})_3\text{Cl}(\text{aeip})$ {aeip=2-(anthracen-9-yl)-1-ethyl-imidazophenanthroline [Liu et al., 2008]. In the native state this complex does not exhibit

fluorescence, however in presence of singlet oxygen it becomes highly fluorescent after excitation at 410nm.

Chemiluminescent probes may also be used to detect singlet oxygen; these do not require excitation light and emit light spontaneously in the presence of singlet oxygen. One commonly used example is 2-methyl-6-phenyl- 3,7-dihydroimidazo [1,2-a] pyrazin-3-one (CLA), and its derivatives MCLA and FLCA [Zhu et al. 2004]. All of these compounds emit light spontaneously in the presence of singlet oxygen. However, they also react with superoxide anion, so their utility is limited.

The $^1\Delta_g$ state of singlet oxygen is paramagnetic and can be detected in the gas phase using EPR spectra [Falick *et al.*, 1965]. Recorded spectrum of singlet oxygen is an almost symmetrical quartet in the region of 9244 MHz. It is well known that cyclohexene is able to react with singlet oxygen. In this reaction the major product is 2-hydroperoxyl cyclohexene. The formation of 2-hydroperoxyl cyclohexene could be monitored by NMR spectroscopy. ^1H NMR spectra of 2-hydroperoxyl cyclohexene exhibit characteristic signal at 4.49ppm for allylic proton, 6.0 and 5.74ppm (doublet) for two vinyl protons, and 8.5 ppm for peroxide-H [DOI: 10.1039/c3tb20806k]. Another useful technique for detection of singlet oxygen is EPR measurement [DOI: 10.1111/php.12557]. As sensor could be used 2,2,6,6-tetramethylpiperidine – TEMP molecule. TEMP is nonparamagnetic compound, however after interaction with singlet oxygen it was transformed into paramagnetic adduct 2,2,6,6-tetramethylpiperidine-n-oxyl radical – TEMPO. The EPR spectrum of TEMPO consist of three equally intense lines. Intensity of spectral line are proportional to amount of generated singlet oxygen.

3. Applications of noble metal nanoparticles in photodynamic therapy

Noble metal nanoparticles exhibit many advantages in comparison with organic photosensitizers. Nanoparticles are much more stable under irradiation than organic dyes; organic dyes can decompose under intense irradiation leading to reduced reaction rates, and gold or silver nanoparticles exhibit significantly higher extinction coefficients than standard organic photosensitizers.

Photofrin is one of the most commonly used photosensitizer. There are several limitations of this compound. The maximum of absorption of this compound is at 630nm. This spectral region is below the biological transparent window. Also molar absorption coefficient at 630nm is low (c. $1170 \text{ M}^{-1}\text{cm}^{-1}$). Therefore, high concentrations of photosensitizer and light must be delivered to tumor. Photofrin does not exhibit high selectivity for tumor tissue, and has a complicated structure which is difficult to synthesize and therefore expensive. Noble metal nanoparticles have significantly higher absorption coefficients, for example: gold nanoechinus $10^{12} \text{ M}^{-1}\text{cm}^{-1}$ [DOI: 10.1002/adma.201400703] or gold nanoshell $10^9 \text{ M}^{-1}\text{cm}^{-1}$ [<http://dx.doi.org/10.1016/j.biomaterials.2014.03.065>]. This difference in absorption coefficient means that it is possible to reduce the power of the excitation light. Organic photosensitizers are known to easily undergo enzymatic degradation, in contrast to noble metal nanoparticles which are stable. Additionally the human body exhibits a biological window from 650 to 1350 nm. This region can be divided into smaller parts: The first biological window (I) has a range from 650 to 950nm, the second biological window (II) is located in the range 1000 – 1350nm, and the third (III) from 1550 to 1870nm. Within these wavelengths the maximum depth of penetration in tissue can be achieved. However, tissue components can also absorb light in this region: (i) In the short-wave region two types of hemoglobin exhibit absorption bands: Deoxyhemoglobin absorbs light at 420 and 580nm, while oxyhemoglobin absorbs light at 410, 550 and 600nm (ii) In this spectral region melanin also absorbs light, although its spectrum shows a continuous character (iii) fat absorbs light with a

maximum absorption at c. 930nm. Thus, the highest transparency exhibited by human tissue is in the range from 800 - 1350nm. In case of noble metal nanoparticles it is possible to control the surface plasmon resonance (SPR) band depending on size and shape of nanoparticles, for example, gold nanorods depending on aspect ratio exhibit SPR over 950nm. A similar situation could be observed in case of gold bipyramids. Moreover, noble metal nanoparticles could be suspended in any organic or non-organic solvent.

3.1 Gold nanoparticle photosensitizers

It was first demonstrated in 2014 that gold nanorods could be used in PDT [DOI: 10.1002/smll.201302719]. It was shown that gold nanorods excited by NIR (915nm, 130mW/cm²) light could generate singlet oxygen and could completely destroy B16F0 melanoma tumors in mice without addition of any organic photosensitizer. During illumination of the gold nanorods with NIR light strong fluorescence could be observed using the SOSG sensor. Illumination with 550nm (130mW/cm²) light showed no signal above background. However, irradiation with 550nm light showed a strong local temperature increase; the basis of photothermal therapeutic (PTT). Despite this, further research proved that PDT is much more effective on the destruction of tumor than PTT therapy. It was observed that gold nanorod mediated PTT (and organic photosensitizer mediated PDT) treatment can only suppress the growth of tumor for short time, whereas gold nanorod mediated PDT could completely destroy solid tumours even under low light doses. Analysis of tissue dissected from other organs such as the liver or spleen did not show noticeable damages after PDT. It was estimated that PDT using gold nanorods is at least 10 times more efficient than conventional anticancer drugs such as doxorubicin. Furthermore, the very low light doses make it possible to use an LED array instead of high power lasers.

While the gold nanorods effectively worked as photosensitizers they were only active in Biological window I. A gold nanorod structure showed exceptionally high extinction coefficients ($\sim 10^{12} \text{ M}^{-1}\text{cm}^{-1}$) in the NIR region (800 – 1700nm) covering both biological windows I and II [DOI: 10.1002/adma.201400703]. During irradiation with 940nm light, singlet oxygen was detected with SOSG, and of particular importance the fluorescence signal was more intense when irradiated with 940nm light than 540nm. Additionally, the results clearly revealed that cellular death caused by the phototoxicity of nanorod gold nanostructures was much higher in cancerous HeLa cells than in noncancerous NIH-3T3 fibroblast cells. These differences arise from the different abilities of the cells to withstand oxidative stress. Due to the exceptionally high extinction factor of the nanoparticles, laser powers adopted in this study were 2-3 times lower than the standards set by American National Standards Institute (ANSI) for skin burning (808nm @ 330mW/cm², 915nm @ 340 mW/cm², 1064nm @ 420 mW/cm², with exposure times from 10 to 1000 seconds). In the gold nanorod study the laser power was set to 130 mW/cm² for all laser wavelengths (880, 915, and 1064nm).

While the above experiments were performed with continuous wave lasers it has been demonstrated that 40nm spherical gold nanoparticles with SPR peak at 524nm, showed greater singlet oxygen generation when the 532nm laser light was pulsed [DOI: 10.1002/smll.201301365]. This could lead to an increased yield of PDT for noble metal nanoparticles, however due to absorption peak at 524nm this solution could be applied in real PDT treatment.

Gold bypyramids have the useful property that by extending or reducing the length of the bypyramid it is possible to change the SPR peak position [10.1039/c5ra15362j]. Depending upon the geometry they can exhibit a maximum absorption in the range 660 to 930nm. Research showed that maximum efficiency of the process was observed when the laser wavelength overlapped with the SPR peak of gold bypyramids. In all experiments lasers power were fixed at 200mW/cm². It was observed that gold bypyramids with SPR peak located at 820nm lead to a significantly higher reduction of the oxygen sensor ABDA peak compared to using methylene blue as photosensitizer when excited with 820nm laser irradiation.

C. Jiang et. al presented that also aggregates gold nanoparticles could be applied as photosensitizer in PDT [dx.doi.org/10.1021/am4007403]. They examined two kind of gold nanoparticles: spherical and rods. Spherical gold nanoparticles with average diameter of 40nm with SPR band at 529nm were prepared by citrate reduction method. Gold nanorods were prepared by CTAB – assister method. Different aspect ratio was obtained by control the amount of added silver nitrate to growing solution.

Plasmonic coupling of gold nanoparticles has been shown for spherical and rod shaped nanoparticles, by the addition of cysteine during synthesis. Cysteine is an amino acid containing a thiol group (-SH) which can easily be attached to metallic surfaces *via* an S – Au bond. In acidic environments cysteine is zwitterionic and therefore could be connected to the surface of other nanoparticles *via* electrostatic interactions, leading to the coupling of gold nanoparticles. Immediately, after the addition of cysteine to a solution containing spherical nanoparticles, the colour changes from red to violet. The UV-Vis spectrum also changes; the SPR band at 529nm is decreased, and simultaneously there is the formation of a new band in the longer wavelength region. This indicates the formation of gold nanoaggregates. The same phenomenon occurs with gold nanorods. The solutions were irradiated with a by femtosecond 800nm laser beam (average beam area 0.3cm², 3 W/cm²), with 60fs pulse and 1 kHz frequency. The generation of singlet oxygen was observed in both unaggregated and aggregated gold nanoparticles, but the singlet oxygen detected was 8.3 times higher with aggregated spherical nanoparticles in comparision with isolated ones. A similar effect was observed in the case of aggregated nanorods, where formation of singlet oxygen was 1.8 times more efficient that in case of unaggregated gold nanorods. In general aggregation of noble metal nanoparticles is seen as negative process, leading to reduce optical properties of nanoparticles, however, this study showed that aggregation of gold nanoparticles could increase formation of singlet oxygen, therefore increasing potential biological applications.

In addition to spheres, and rods, hollow gold nanoparticles were investigated in the form of gold nanocages, spherical hollow nanoparticles and nanorods in shell [http://dx.doi.org/10.1016/j.biomaterials.2014.03.065]. It was estimated that molar extinction coefficients at 808nm increased in the following order: spherical hollow nanoparticles, nanorods in shell, gold nanorods and gold nanocages. Gold nanoshells exhibited a strong SPR peak upto 1100nm which is within the biological transparency window. The gold nanoshells could sensitize singlet oxygen after NIR light activation (850 - 1000nm), but not with visible light. When used *in vitro* experiment against HeLa cells significant amounts of cell death was seen after irradiation. However, the percentage cell viability was almost 3.4 times lower in the case of irradiation with 940nm (54mW/cm²) laser light compared to 540nm (28mW/cm²) light. The decrease in efficacy was due to the low amount of singlet oxygen formed upon irradiation at 540nm. In order to confirm that cellular death were caused by

singlet oxygen, the well known ROS quencher sodium azide were added to samples. Sodium azide were significantly increases the viability of HeLa cells with irradiation by 940nm light, but there was no change in the case of 550nm irradiation. This confirmed that cellular death after NIR irradiation was connected with the presence of singlet oxygen, whilst in case of 550nm the smaller amount of cellular death was caused by a photothermal effect. The efficacy of the gold nanocage particles was also investigated in mice on the destruction of B16F0 melanoma tumors with irradiation by 808nm (150mW/cm² by 13 minutes) and 980nm (150mW/cm² by 10 minutes) laser light. Results showed a significant decrease in the size of the tumour in the mice for both wavelengths of light. Of particular note, the laser powers used were almost 3 times lower than the standard of the American National Standards Institute for skin burning (808nm = 330mW/cm²; 980nm = 360mW/cm²) with exposure time 10 - 1000 seconds.

3.2 Alternative metal nanoparticle photosensitizers

Gold and silver nanoparticles have been shown to generate singlet oxygen, although their properties are dependent upon their morphology [DOI: 10.1039/c3tb20806k]. It was observed that irradiation with 885nm laser light of silver decahedron and silver nanoprisms lead to formation of singlet oxygen, whereas no singlet oxygen was detected with silver nanocubes. A similar phenomenon was observed for gold nanoparticles. In the work described the wavelength of the laser light did not overlap with the SPR band of the nanoparticles. However, irradiation of silver decahedrons (SPR band c.a. 520nm) by NIR 885nm laser light results in very strong singlet oxygen phosphorescence signal, whereas irradiation of gold decahedrons in same conditions do not results in formation of singlet oxygen. Similarly, irradiation of silver nanoprisms (SPR band c.a 590nm) by 544 laser light results in formation of singlet oxygen, whilst irradiation of silver nanocubes (SPR band c.a 500nm) by 525 nm laser light lead to weak generation of singlet oxygen, even though SPR band of nanoparticles and laser light overlaps. Therefore, authors assumed that generation of singlet oxygen in the prescene of noble metal nanoparticles strongly depend on their morphology. Theoretical calculation predicts that molecular oxygen could be adsorbed on Au(111), Au(110) and Au(100) surfaces. However, in case of Au(111) and Au(100) oxygen mostly exist in the atomic form. Only in case of Au(110) crystalline face molecular oxygen do not dissociate and could be excited during irradiation to singlet oxygen. In case of silver nanoparticles calculation and experimental techniques shown that molecular oxygen could be adsorbed on Ag(100), Ag(110) and Ag(111) surfaces. However, in case of Ag(100) and Ag(110) surfaces adsorbed oxygen molecule will dissociate into atomic form. Therefore, singlet oxygen could be only photosensitized form the Ag(111) crystalline faces, but not on the Ag(100) and Ag(110). Above relationship may not work perfectly in some cases, due to some defects in shapes of nanoparticles. For example, distorted nanocubes may contain small amount of 110 or 111 faces where singlet oxygen might be able to be photosensitized. The key factor which allow to applied noble metal nanoparticles in PDT is it morphology and selective molecular binding of oxygen molecule to different crystallographic faces. In case of silver nanoparticles singlet oxygen could be formed only on Ag(111) surfaces. Therefore, singlet oxygen could be formed in case of silver decahedrons or nanoprisms, but not in case of silver nanocubes. In case of gold nanoparticles singlet oxygen could be formed only from Au(110) surfaces. Therefore, gold nanorods or bypyramids could be applied, wheres gold decahedron could not generate singlet oxygen.

It is also possible to use semi – conductor nanoparticles as photosensitizers provided that they have a higher energy band gap than that of singlet oxygen. One example uses tungsten oxide nanowires as a

semi-conductor photosensitizer since the the energy band gap in $W_{18}O_{49}$ nanowires is approximately 1.26eV, which is higher than energy band gap of singlet oxygen 0.97eV, making energy transfer from the surface of the tungsten oxide to molecular oxygen possible [DOI: 10.1002/ange.201307358]. Excitation of $W_{18}O_{49}$ was obtained after irradiation by 980nm light. The molar extinction coefficient was estimated to be 0.5×10^7 at 980nm which is almost three orders of magnitude higher than the extinction coefficient of some organic photosensitizers. While singlet oxygen could be detected under irradiation by 980nm light using SOSG, no fluorescence was detected after irradiation by 808nm. This is due to the insufficient energy of the photons which could not therefore excite the tungsten oxide nanowires. The nanowires were also used to treat B16F0 melanoma tumors in mice under low power laser irradiation (980nm – 200mW/cm²), most probably by PDT, and not PTT.

3.3 Metal composite nanoparticles

While it has been shown that metal nanoparticles can be effectively used for PDT, the incorporation of an organic sensitizer can enhance the properties of the particle. Gold nanostars were prepared due to their absorption band in the near infrared spectral region, and coated with a silica layer to encapsulate the organic photosensitizer methylene blue in a shell around nanoparticles [doi:10.1021/la202602q]. Fluorescence of SOSG was observed even in the case of irradiation by 633nm laser light with extremely low power (8mW). It was observed that these particles produces significantly more singlet oxygen than silica-coated gold nanostars without embedded MB. It should be noted that no photothermal effects were observed due to the relatively low laser power (700mW/cm²) and application of 633nm light which did not overlap with the SPR band of gold nanostar (800nm). It was also demonstrated that MB-loaded nanostars exhibited cytotoxic effect on BT549 breast cancer cells.

Gold has also been used in conjunction with 5-aminolevulinic acid (5-ALA), a precursor of photoporphyrin IX, which is widely used as photosensitizer in clinical applications [https://www.futuremedicine.com/doi/full/10.2217/17435889.3.6.777]. 5-ALA possesses many useful properties such as low toxicity (before excitation), rapid excretion from the body, and rapid conversion to porphyrins. The main disadvantage of 5-ALA is the zwitterionic character which significantly limits tissue penetration. In this study 5-ALA molecules were conjugated to the surface of the gold nanoparticles surfaces, whereby the nanoparticles could be used as transporter. At physiological pH, 5-ALA is negatively charged and it can bind to the positively charged gold surface by electrostatic interaction. The particles were tested against fibrosarcoma cells, where a significant increase in singlet oxygen was observed. Irradiation were carried out by a broadband 150W halogen lamp for 1 minute, and c. 50% more cancer cells were killed in the case of 5-ALA conjugated to gold nanoparticles, compared to standard application of 5-ALA molecules alone. Even more significant is the fact that in a co-culture system with fibrosarcoma cells, normal fibroblast cells only suffered a minimal effect from the singlet oxygen.

The proporphyrin IX (PpIX) molecule itself was also used to functionalize Ag@SiO₂ core-shell nanoparticles [DOI: 10.1111/php.12557]. The highest efficiency of oxygen generation was gained with 100nm spherical silver nanoparticles with a 6nm thick silica layer containing the PpIX. The amount of singlet oxygen formed was approximately 1.2 and 3.7 times higher than in case of free PpIX molecules and silica nanoparticles functionalized by PpIX, respectively. Further increases in the thickness of the silica layer reduced the activity; to levels even lower than for free PpIX solutions. The authors

attributed the increased efficiency in the generation of singlet oxygen on the strong electromagnetic force generated by the silver nanoparticles during irradiation. Increasing the distance between the surface of the silver and the PpIX molecules reduces the effective electromagnetic field acting on the photosensitizer molecule and causes a decrease in the yield of the reaction. The authors also underline the importance of the overlap between absorption band of PpIX and SPR band of silica nanoparticles.

Gold nanoparticles have also been investigated after being conjugated with the organic photosensitizer phthalocyanine [DOI: 10.1039/b602830f]. Phthalocyanine and its zinc derivatives have been successfully used in photodynamic treatment, however the hydrophobic character of the phthalocyanine impedes its delivery. It was shown that gold nanoparticles with an average diameter of 2-4nm could be functionalized to deliver the organic photosensitizer into tumour cells. When the photosensitizer was bound to the gold surface the quantum yield of singlet oxygen generation was 0.65, compared with 0.45 for the free photosensitizer. The gold nanoparticles conjugated with phthalocyanine were shown to be effective against HeLa cells where significant cell mortality through PDT was observed. Furthermore, the conjugation of the photosensitizer to the nanoparticle increases the selectivity and biodistribution.

Similar research presenting applications of phthalocyanine derivatives conjugated to noble metal nanoparticles were presented by Ke *et al* [2014]. In this work they attached tetra – substituted carboxyl aluminium phthalocyanine (AlC₄Pc) to the surface of spherical gold nanoparticles coated with a SiO₂ layer. The distance between the AlC₄Pc moiety and the gold surface could be controlled by changing the thickness of silica layer. Optical distance was found at 10.6 nm. In that case generation of singlet oxygen was 2.1 time higher than in case of the free AlC₄Pc solution. Formation of singlet oxygen was monitored by ABDA. Irradiation was carried out by 680nm LED lamp with average power 10mW/cm² by 40minutes.

Gold clusters have also been used for PDT. The Au₂₅(SR)₁₈⁻ cluster (where SR is general symbol for molecules with thiol group) was either water or organic soluble depending on the exact chemical character of SR part of cluster [dx.doi.org/10.1021/cm500260z]. The cluster was modified with either phenylethanethiol Au₂₅(PET)₁₈⁻ or captopril Au₂₅(Capt)₁₈⁻. The Au₂₅(PET)₁₈⁻ cluster was found to be only soluble in organic liquids which limits its applications in clinical PDT. It was observed that Au₂₅(Capt)₁₈⁻ clusters generated significantly more singlet oxygen than the organic compound methylene blue (Irradiation at 650nm (13mW/cm²) and 808nm (41mW/cm²)). To confirm high biocompatibility and efficient singlet oxygen generation, the Au₂₅(Capt)₁₈⁻ cluster was tested in HeLa cancer cells. Results showed that the viability of HeLa cells incubated with the Au₂₅(Capt)₁₈⁻ cluster was drastically reduced after irradiation by 808nm laser light. The authors considered two possible mechanism of death cells: photothermal and photocytotoxic effect by singlet oxygen. To determine the mechanism the singlet scavenger, histidine, was added to the sample. It was observed that cell viability was significantly increased in the presence of histidine; indicating that the cancer cells were damaged and killed in most cases after interaction with singlet oxygen molecules.

Summary of application of noble metal nanoparticles in PDT in various experimental conditions

Nanoparticles	Laser wavelenght [nm]	Power intensity	Method of detection	Target cells	Ref
Au nanorods	915	130mW/cm ²	SOSG	B16F0	
Au nanoechinus	940	130mW/cm ²	SOSG	HeLa	
Au bypiramids	660 710 820 930	200mW/cm ²	ABDA	HeLa	
Aggregated Au nanoparticles	800	3W/cm ²	ABDA	-	
Au nano shell	808	150mW/cm ²	direct phosphorescence at 1063nm	Hela	
	980		SOSG	B16F0	
Ag nanoprisms	544	45mw/cm ²	SOSG, hydroperoxidation of cyclohexene	-	
Ag decahedrons	885	66mW/cm ²			
W18O49 nanorods	980	200mW/cm ²	SOSG	B16F0	
Au nanostar@SiO ₂ @methylene blue	633	700mW/cm ²	SOSG	BT549	
Au@SiO ₂ @AIC ₄ Pc	680	10mW/cm ²	ABDA	-	
Ag@SiO ₂ @PpIX	halogen white lamp	30W	TEMP	-	
Au ₂₅ (capt)18- cluster	650	13mW/cm ²	DAB	Hela	
	808	41mW/cm ²			

4. Conclusions

In this article we have described the applications of noble metal nanoparticles in photodynamic therapy (PDT) and possible detection methods of the singlet oxygen generated. Noble metal nanoparticles exhibit a number of desirable properties for use in PDT. Firstly, they are able to generate singlet oxygen during irradiation by light in the range 800 – 1000 nm where human tissue exhibits a transparency window. In comparision with typical organic photosensitizers such as hematoporphyrins they exhibit higher photostability and resistance to enzymatic degradation. Also, higher excitation coefficients could enable a reduction in the excitation power of light. It is expected that due to their optical properties, methods based on noble metal nanoparticles will significantly impact upon the detection and treatment of cancer.

Acknowledgements

References

Meyer–Betz, F. Untersuchungen über die biologische photodynamische Wirkung des Hematoporphyrins und anderer Derivative des Blut und Galenafarbstoffs. Dtsch Arch. Klin. 112, 476–503 (1913)

[Schwartz, S. K., Abolon, K. & Vermund, H. Some relationships of porphyrins, X-rays and tumors. Univ. Minn. Med. Bull. 27, 7–8 (1955).]

Lipson, R. L., Baldes, E. J. & Olsen, A. M. The use of an derivative of hematoporphyrin in tumor detection. J. Natl Cancer Inst. 26, 1–11 (1961);

Lipson, R. L. & Baldes, E. J. The photodynamic properties of a particular hematoporphyrin derivative. Arch. Dermatol. 82, 508–516 (1960).

Diamond, I. et al. Photodynamic therapy of malignant tumours. Lancet 2, 1175–1177 (1972).

Dougherty, T. J., Grindey, G. B., Fiel, R., Weishaupt, K. R. & Boyle, D. G. Photoradiation therapy. II. Cure of animal tumors with hematoporphyrin and light. J. Natl Cancer Inst. 55, 115–121 (1975).

Kelly, J. F., Snell, M. E. & Berenbaum, M. C. Photodynamic destruction of human bladder carcinoma. Br. J. Cancer 31, 237–244 (1975).

Kelly, J. F. & Snell, M. E. Hematoporphyrin derivative: a possible aid in the diagnosis and therapy of carcinoma of the bladder. J. Urol. 115, 150–151 (1976)

Hayata, Y., Kato, H., Konaka, C., Ono, J. & Takizawa, N. Hematoporphyrin derivative and laser photoradiation in the treatment of lung cancer. Chest 81, 269–277 (1982).

; Balchum, O. J., Doiron, D. R. & Huth, G. C. Photoradiation therapy of endobronchial lung cancers employing the photodynamic action of hematoporphyrin derivative. Lasers Surg. Med. 4, 13–30 (1984).],

[Hayata, Y., Kato, H., Okitsu, H., Kawaguchi, M. & Konaka, C. Photodynamic therapy with hematoporphyrin derivative in cancer of the upper gastrointestinal tract. Semin. Surg. Oncol. 1, 1–11 (1985).]

[Sandeman, D. R. Photodynamic therapy in the management of malignant gliomas: a review. Lasers Med. Sci. 1, 163–167 (1986);

Hill, J. S. et al. Selective uptake of hematoporphyrin derivative into human cerebral glioma. Neurosurgery 26, 248–254 (1990);

Popovic, E. A., Kaye, A. H. & Hill, J. S. Photodynamic therapy of brain tumors. *J. Clin. Laser Med. Surg.* 14, 251–261 (1996);

Rosenthal, M. A. et al. Phase I and pharmacokinetic study of photodynamic therapy for high-grade gliomas using a novel boronated porphyrin. *J. Clin. Oncol.* 19, 519–524 (2001).], head and neck tumor

[Schweitzer, V. G. Photodynamic therapy for treatment of head and neck cancer. *Otolaryngol. Head Neck Surg.* 102, 225–232 (1990);

Biel, M. A. Photodynamic therapy and the treatment of head and neck neoplasia. *Laryngoscope* 108, 1259–1268 (1998).]

MLkvy, P. et al. Photodynamic therapy for gastrointestinal tumors using three photosensitizers — ALA induced PPIX, Photofrin and MTHPC. A pilot study. *Neoplasma* b45, 157–161 (1998).

Falick, A.M., Mahan, B.H., and Myers, R.J., *J. Chem. Phys.*, 1965, vol. 42, no. 5, p. 1837.

G.R. Martines, J.L. Ravanat, M.H.G. Medeiros, J. Cadet, P.D. Mascio, *J. Am. Chem. Soc.* 122 (2000) 10212.

[38] G.R. Martinez, J.L. Ravanat, J. Cadet, S. Miyamoto, M.H.G. Medeiros, P.D. Mascio, *J. Am. Chem. Soc.* 126 (2004) 3057.,

[39] M. Botsivall, D.F. Evans, *J. Chem. Soc. Chem. Comm* (1979) 1114.

[40] V. Nardello, J.M. Aubry, P. Johnston, I. Bulduk, A.H.M. de Vries, P.L. Alsters, *Synlett* 17 (2005) 2667.

[41] V. Nardello, J.M. Aubry, *Tetrahedron Lett.* 38 (1997) 7361.

[42] G.R. Martinez, F. Garcia, L.H. Catalani, J. Cadet, M.C.B. Oliverira, G.E. Ronsein, S. Miyamoto, M.H.G. Medeiros, P.D. Mascio, *Tetrahedron* 62 (2006) 10762.

[43] V. Nardello, N. Azaroual, I. Cervoise, G. Vermeersch, J.M. Aubry, *Tetrahedron* 52 (1996) 2031.].

Ke, X., Wang, D., Chen, C. et al. *Nanoscale Res Lett* (2014) 9: 666. <https://doi.org/10.1186/1556-276X-9-666>

N. Umezawa, K. Tanaka, Y. Urano, K. Kikuchi, T. Higuchi, T. Nagano, *Angew. Chem., Int. Ed. Engl.* 38 (1999) 2899

K. Tanaka, T. Miura, N. Umezawa, Y. Urano, K. Kikuchi, T. Higuchi, T. Nagano, *J. Am. Chem. Soc.* 123 (2001) 2530.

C. Flors, M.J. Fryer, J. Waring, B. Reeder, U. Bechtold, P.M. Mullineaux, S. Nonell, M.T. Wilson, N.R. Baker, J. Exp. Bot. 57 (2006) 1725

B. Song, G.L. Wang, M.Q. Tan, J.L. Yuan, J. Am. Chem. Soc. 128 (2006) 13442.

M.Q. Tan, B. Song, G.L. Wang, J.L. Yuan, Free Radical Biol. Med. 40 (2006) 1644

Y.J. Liu, K.Z. Wang, Eur. J. Inorg. Chem. 2008 (2008) 5214

Y.J. Liu, K.Z. Wang, Eur. J. Inorg. Chem. 2008 (2008) 5214

D.B. Zhu, D. Xing, Y.D. Wei, X. Li, B. Gao, Luminescence 19 (2004) 278